

Intelligent torque observer combined with backstepping sliding-mode control for two-mass systems

Vo Thanh Ha¹, Pham Thi Giang²

¹Faculty of Electrical and Electrical Engineering, University of Transport and Communications, Hanoi, Vietnam

²Faculty of Electrical Engineering, University of Economics-Technology for Industries, Hanoi, Vietnam

Article Info

Article history:

Received Aug 22, 2021

Revised Aug 26, 2022

Accepted Sep 11, 2022

Keywords:

Backstepping method

High-gain observer

RBF-neural network

Sliding mode control

Two-mass system

ABSTRACT

The construction of a backstepping-sliding mode control using a high-gain observer's neural network for torque estimation is presented in this research. The correctness of the load torque data is crucial to solving the two-mass system control issue. The article suggests a radial basis function neural network topology to handle load torque estimation. When a non-rigid drive shaft is present, the predicted value is merged with backstepping-sliding mode control to ensure speed tracking performance. The closed-stability loop is demonstrated analytically and quantitatively to prove it. Additionally, a high-gain observer-based structure is used to compare the effectiveness of the proposed control. The effectiveness of the proposed control structure is demonstrated by MATLAB simulation.

This is an open access article under the [CC BY-SA](https://creativecommons.org/licenses/by-sa/4.0/) license.



Corresponding Author:

Vo Thanh Ha

Faculty of Electrical and Electrical Engineering, University of Transport and Communications

No. 3, Cau Giay district, Ha Noi city, Vietnam

Email: vothanhha.ktd@utc.edu.vn

1. INTRODUCTION

The challenge of speed tracking control in a dual mass system with flexible driving shafts is examined in this work. The stability of the two-mass system is reduced by this unsolved issue when operating over the whole speed spectrum, but notably in the low-speed range [1] and [2]. The target is to lessen the effects of disturbances to the moment of inertia, torque, and soft coupling, impacting the quality of this two-mass system. Therefore, this system needs a control method or mechanical solution is required. There are speed control techniques for the two-mass system (TMS) in use right now, including PID, PI-D, sliding mode, flatness-based, backstepping, fuzzy, and more. Because of its ease of controller construction and parameter change, PID controllers are frequently used in traditional management [3].

Nevertheless, the PID controller is constrained to a few operational areas since the two-mass system is a nonlinear drive system. In the other works [4], and [5], optimization techniques are used to develop the digital modified-IPD (m-IPD) controller for the speed loop of a two-mass system. The driving mechanism, therefore, reacts to the specified load speed precisely. Additionally, the flux and rate of the elastic coupling drive system are controlled using flatness-based control in [6]–[8]. The drive mechanism can run in a weakening field area and the entire base speed range. According to the simulation's findings, the drive system can produce quick and precise reactions (flux, speed, torque) and prevent mechanical oscillation.

On the other hand, the flux and speed of the system are controlled via the backstepping control method in [9], and [10]. The simulation findings demonstrate the suppression of the drive's mechanical oscillation; nonetheless, speed response experiences delay in reaction to changes in system parameters. *Azzaoui et al.* [11] also provided a design strategy for a speed load fuzzy controller to lessen vibration for three mass resonance

systems. This controller reduces shaft oscillation. On the other hand, the controller hasn't been examined and tested for resilience when interference affects the drive system. In other drive applications, slide mode control (SMC) is a practical, straightforward nonlinear control method. However, this controller needs knowledge about the system, the upper bounds of the uncertainty components, and the inevitable chattering phenomena [12]. Various control techniques mentioned earlier sought to lessen torsional vibrations at the shaft. In addition, when designing controls for TMS, all state variables are often assumed to be available [13]-[16].

The estimate of state variables for the two-mass system, such as moving horizon estimation, Luenberger, Kalman filter, and neural network, is actively researched to improve the control system's performance and simplify the control structure. The fundamental issue is that during the operation of this drive system, it is challenging to estimate the state variable precisely. Ikeda and Hanamoto [17] discusses the challenges of using tools to estimate horizon movement and rebuild state variables while enhancing the control structure of a two-mass MHE system. Korondi *et al.* [18], a modified fuzzy Luenberger Observer is used to identify necessary dynamic states based on the inaccuracy between the reference and estimator outputs, the other discrepancies between electromagnetic and shaft torque, and its derivatives. Fuzzy systems use these signals to establish where the observer poles are [18].

The benefits of the Kaman filter with time-varying parameters can also be viewed as system noise and taken into account while designing. Therefore, this filter has the potential to be more effective than Luenberger observers in terms of parameter identification. Additionally, they appear well adapted when it comes to simultaneous estimation of physical parameters and states, which calls for an adjustment of feedback gain [19]. Currently, [20]–[22] network's ability to adapt makes them effective instruments for sensing system states without any prior understanding of the dynamics of the system. This study gives radial basis function neural network observer estimations of the load moment (RBF-NN). In flexible joint manipulators, the research [23] and [24] uses a nonlinear neural network in its parameterization. Without a previous understanding of system dynamics, the observer demonstrates its benefits while interacting with the highly nonlinear system.

This study introduces a backstepping-sliding mode controller with an RBF neural network (RBF-NN) observer for the speed loop to achieve accurate angular speed matching with the angular reference speed. Additionally, because the torsion shaft dynamics are taken into account in aggregate control, a control strategy based on this model may considerably enhance the performance of the transmission system, such as control precision and torsional oscillation reduction. Finally, simulations validate the viability and efficacy of the suggested approach.

The remainder of the essay is organized as follows. The driving system modelling is shown in the first part. The second section demonstrates how RBF-NN handles the load torque observer while backstepping-sliding mode control is used to create the speed control loop. The high-gain load torque observer based on backstepping sliding mode control is presented in the third part for comparison and evaluation with the RBF-NN observer. The simulation results in the final part demonstrate the effectiveness of the control mechanism before some recommendations and viewpoints are offered.

2. MODELING OF A TWO-MASS-SYSTEM

Typical structure of a two-mass system is shown in Figure 1 and Figure 2. The drive system can be described by the following linear dynamical in (1) [25].

$$\begin{cases} \dot{\omega}_L = \frac{1}{J_L} (T_s - T_L) \\ \dot{T}_s = K_s (\omega_M - \omega_L) \\ \dot{\omega}_M = \frac{1}{J_M} (T_e - T_s) \end{cases} \quad (1)$$

Where ω_M, ω_L are motor speed, load speed; T_e, T_L and T_s are motor, load and shaft torque, respectively; B_s is shaft damping coefficient; K_s is shaft stiffness; J_L is inertia load torque.

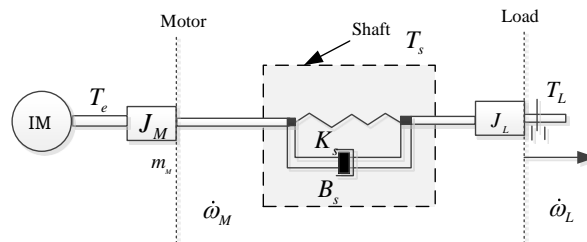


Figure 1. Structure of a two-mass system

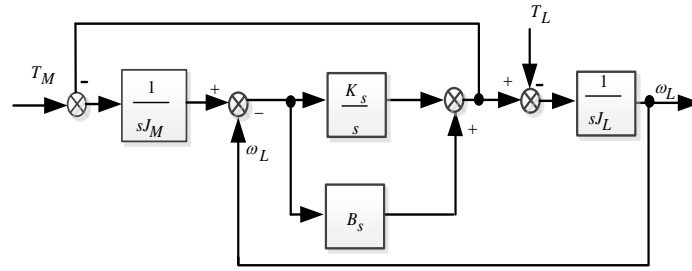


Figure 2. Structure of the mathematical model of a TMS

3. DESIGN OF BACKSTEPPING-SLIDING MODE CONTROLLER COMBINED WITH INTELLIGENT TORQUE OBSERVER

According to Lyapunov's theory, the backstepping design approach often considers the entire system's stability. Therefore, accurate mathematical modelling is necessary to regulate the disturbance. The controller is integrated with the neural network load torque observer to solve the issue by updating the weight value. The architecture of the neural network load torque observer and backstepping-sliding mode control may be summed up as:

- i) Step 1: Determining reference shaft torque

In this step, the tracking error for actual motor angular speed with reference motor angular speed is defined as (2):

$$e_L = \omega_L - \omega_{Ld} \tag{2}$$

Where ω_L, ω_{Ld} are actual and reference load angular speeds. Consider the following positive definite Lyapunov function for this step with V_1 function is chosen as (3):

$$V_1 = \frac{1}{2} e_L^2 \tag{3}$$

The derivative of in (3) gives:

$$\dot{V}_1 = e_L \dot{e}_L = e_L (\dot{\omega}_L - \dot{\omega}_{Ld}) = e_L \left(\frac{1}{J_L} (T_s - T_L) - \dot{\omega}_{Ld} \right) \tag{4}$$

From in (4), taking T_{sd} as the virtual control, it is suggested that the reference shaft torque is designed as (5):

$$T_{sd} = \hat{T}_L - J_L (-\dot{\omega}_{Ld} + c_1 e_L) \tag{5}$$

Where \hat{T}_L is load torque estimation which is provided by the neural network; c_1 is a positive coefficient.

- ii) Step 2: Determining reference load angular speed.

Shaft torque error e_{Ts} is defined as (6):

$$e_{Ts} = T_s - T_{sd} \tag{6}$$

Substituting in (5) into in (4) result`s in (7):

$$\dot{V}_1 = e_L \left(\frac{1}{J_L} (e_{Ts} + T_{sd} - T_L) - \dot{\omega}_{Ld} \right) = -c_1 e_L^2 + \frac{1}{J_L} e_L e_{Ts} + \frac{1}{J_L} e_L (\hat{T}_L - T_L) \tag{7}$$

The Lyapunov candidate function is chosen at this step as (8):

$$V_2 = V_1 + \frac{1}{2} e_{Ts}^2 \tag{8}$$

Taking the derivative of in (8) gives in (9):

$$\dot{V}_2 = \dot{V}_1 + e_{Ts} \dot{e}_{Ts} = -c_1 e_L^2 + e_{Ts} \left(\frac{1}{J_L} e_L + K_s (\omega_M - \omega_L) - \dot{T}_{sd} \right) + \frac{1}{J_L} e_L (\hat{T}_L - T_L) \tag{9}$$

Based on NN observer, load torque T_L and load torque estimation \hat{T}_L is defined as (10):

$$\begin{aligned}\hat{T}_L &= \hat{W}^T h \\ T_L &= W^T h + \varepsilon\end{aligned}\quad (10)$$

Where W^T is weight value of RBF, \hat{W}^T denotes weight value estimation; h is radial-basis function vector in the hidden layer of RBF; ε is an error. Gaussian function value for neural net i in hidden layer is shown as (11):

$$h_i = \exp\left(-\frac{\|\omega_L - c_i\|}{2b_i^2}\right)\quad (11)$$

Where c_i denotes value of center point of the Gaussian function of neural net i for the i th input, b_i represent the width value of Gaussian function for neural net i . In this case, assuming that ε is ignored leading to $\tilde{W} = \hat{W} - W$. In (9) can be rewritten as (12):

$$\begin{aligned}\dot{V}_2 &= -e_L^2 + e_{T_s}\left(\frac{1}{J_L}e_L + K_s(\omega_M - \omega_L) - \dot{T}_{sd}\right) + \frac{1}{J_L}e_L(\hat{W}^T h - W^T h) \\ &= -e_L^2 + e_{T_s}\left(\frac{1}{J_L}e_L + K_s(\omega_M - \omega_L) - \dot{T}_{sd}\right) + \frac{1}{J_L}e_L\tilde{W}^T h\end{aligned}\quad (12)$$

In (12) indicates that the reference load angular speed is defined as (13):

$$\omega_{Md} = \frac{\dot{T}_{sd} - c_2 e_{T_s}}{K_s} - \frac{1}{J_L K_s} e_L + \omega_L\quad (13)$$

With the virtual control defined as in (13), (12) can be rewritten as (14):

$$\begin{aligned}\dot{V}_2 &= -c_1 e_L^2 + e_{T_s}\left(\frac{1}{J_L}e_L + K_s(\omega_M - \omega_L) - \dot{T}_{sd}\right) + \frac{1}{J_L}e_L(\hat{W}^T h - W^T h) = -c_1 e_L^2 - c_2 e_{T_s}^2 + \\ &\frac{1}{J_L}e_L\tilde{W}^T h\end{aligned}\quad (14)$$

iii) Step 3: In this final procedure, actual control input T_e is designed via the selection of the following surface to increase the robustness of the system. We choose the sliding surface as (15):

$$s = \alpha(\omega_M - \omega_{Md})\quad (15)$$

Where ω_{Md} , ω_M are actual and reference motor angular speed. The Lyapunov candidate function with sliding surface combined with RBF neural network observer is defined as (16):

$$V = V_2 + \frac{1}{2}s^2 + \frac{1}{2}\text{trace}(\tilde{W}^T \Gamma \tilde{W})\quad (16)$$

Then derivative of (16) with respect to time given by (17):

$$\begin{aligned}\dot{V} &= \dot{V}_2 + s\dot{s} + \text{tr}\left(\tilde{W}^T \Gamma \dot{\tilde{W}}\right) = -c_1 e_L^2 - c_2 e_{T_s}^2 + s\alpha\left(\frac{1}{J_M}(T_e - T_s) - \dot{\omega}_{Md}\right) + \\ &\text{tr}\left(\tilde{W}^T\left(\frac{1}{J_L}e_L h + \Gamma \dot{\tilde{W}}\right)\right)\end{aligned}\quad (17)$$

Consequently, the motor torque control law of the two-mass system is chosen as (18):

$$T_e = J_M \dot{\omega}_{Md} + T_s - \frac{J_M}{\alpha}(c_3 \text{sgn}(s) + c_4 s)\quad (18)$$

Where α is a coefficient of the sliding mode control to reach a fast steady-state. The adaptive law of RBF-NN observer is given as (19):

$$\dot{\hat{W}} = -\Gamma^{-1} \frac{1}{J_L} e_L h\quad (19)$$

Then, the derivative of the Lyapunov candidate function (16) results in (20):

$$\dot{V} = -c_1 e_L^2 - c_2 e_{T_s}^2 - c_3 \text{sign}(s)s - c_4 s^2\quad (20)$$

where c_1, c_2, c_3 and c_4 are the positive constant that determine the closed-loop dynamics, as in Table 1. From (21), $\dot{V} \leq 0$, thus the stability of the control system is guaranteed.

Table 1. System parameter

System parameter	Value
J_M	0.1 kgm ²
J_L	0.01 kgm ²
K_s	20 Nm/rad

4. DESIGN OF H-GAIN LOAD TORQUE OBSERVER

For the two-mass systems, a high-gain observer coupled with backstepping-sliding mode control is also examined in addition to the NN observer for estimating load torque disturbance. In (11) and (19), the angular speed error and actual angular speed are all that the NN observer needs to know, but the shaft torque control rule is more important to the high-gain observer. For example, let's say that (1) now reads as (21):

$$\tau = T_s - J_L \dot{\omega}_L \quad (21)$$

$\hat{\tau}$ denotes observed load torque by using HGO, then estimation error of load torque is defined as (22):

$$\tilde{\tau} = \tau - \hat{\tau} \quad (22)$$

The dynamic of observed load torque $\hat{\tau}$ is designed as (23):

$$\dot{\hat{\tau}} = \frac{1}{\varepsilon} (T_s - J_L \dot{\omega}_L - \hat{\tau}) \quad (23)$$

Where $1/\varepsilon$ is observer gain. Load torque estimation error dynamic is given as (24):

$$\dot{\tilde{\tau}} = -\frac{1}{\varepsilon} \tilde{\tau} + \dot{\tau} \quad (24)$$

Combining observed load torque $\hat{\tau}$ with backstepping-sliding mode control, (5) is rewritten as (25):

$$T_{s\tau} = \hat{\tau} - J_L (-\dot{\omega}_{Ld} + c_1 e_L) \quad (25)$$

In order to analyse the stability of the high-gain torque observer-based backstepping-sliding mode control, Lyapunov candidate function V_τ is defined as (26):

$$V_\tau = \frac{1}{2} e_L^2 + \frac{1}{2} \tilde{\tau}^2 + \frac{1}{2} e_{T_s}^2 + \frac{1}{2} s^2 \quad (26)$$

Substituting the law controls (25), (13), and (18) into derivative of (26) results in (27):

$$\dot{V}_\tau = -c_1 e_L^2 + \frac{1}{J_M} e_L \tilde{\tau} + \tilde{\tau} \left(-\frac{1}{\varepsilon} \tilde{\tau} + \dot{\tau} \right) - c_2 e_{T_s}^2 + s \alpha \left(\frac{1}{J_M} (T_e - T_s) - \dot{\omega}_{Md} \right) \quad (27)$$

Then (17) is expressed as (28):

$$\dot{V}_\tau = -\left(c_1 - \frac{1}{J_M} \right) e_L^2 - \frac{1}{J_M} \left(e_L - \frac{\tilde{\tau}}{2} \right)^2 - \left(\frac{1}{2\varepsilon} - \frac{1}{4J_M} \right) \tilde{\tau}^2 - \frac{1}{2\varepsilon} (\tilde{\tau} - \varepsilon \dot{\tau})^2 + \frac{\varepsilon}{2} \dot{\tau}^2 - c_2 e_{T_s}^2 - c_3 \text{sign}(s)s - c_4 s^2 \quad (28)$$

Simplifying (28), we obtain as (29):

$$\dot{V}_\tau \leq -\lambda V + \zeta \quad (29)$$

Where constants λ and ζ satisfy that as (30):

$$\begin{cases} \zeta = \frac{\varepsilon}{2} \dot{\tau}^2 \\ \lambda = \min \left\{ c_1 - \frac{1}{J_M}, \frac{1}{2\varepsilon} - \frac{1}{4J_M}, c_2, c_4 \right\} \end{cases} \quad (30)$$

In (29) implies that the high-gain load torque observer-based backstepping-sliding mode control is input-to-state stability (ISS).

5. SIMULATION RESULTS

Figure 3 depicts the backstepping sliding mode control- neural network control framework for a two-mass system. The target to check the precision and accessibility of the method, the suggested adaptive controller is simulated in the MATLAB/Simulink environment and compared to the model-based strategy. The following are the simulation parameters listed in Table 1. Control value parameter such as $\alpha = 2$; $c_1 = 13$; $c_2 = 65$; $c_3 = 25$; $c_4 = 30$. Furthermore, the RBF neural network observer's parameters are chosen as in Table 2.

Table 2. Observer parameter

System parameter	Value
Γ	$\begin{bmatrix} 3 & \dots & 3 \\ \vdots & \ddots & \vdots \\ 3 & \dots & 3 \end{bmatrix}_{n \times n}$
c	$linspace(-30, 30, n)$
b	0.25

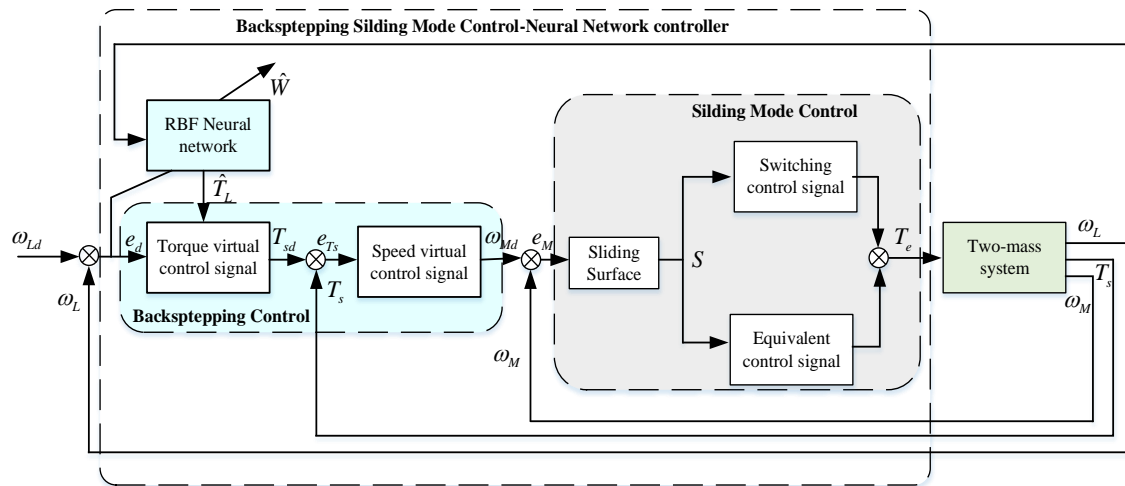


Figure 3. Control structure of B-SMC-NN observer for two-mass system

Figure 4 shows the responses of the two controllers compared to the reference value. It can be seen that backstepping-sliding mode control-neural controller generated an angular load speed that is considerably close to the desired value. However, the unknown factor combined with the disturbance exists in the system. Otherwise, these adverse elements significantly affect the BSMC performance when its load speed is quite different from the reference. Likewise, the angular motor speed results show the corresponding performance in Figure 5.

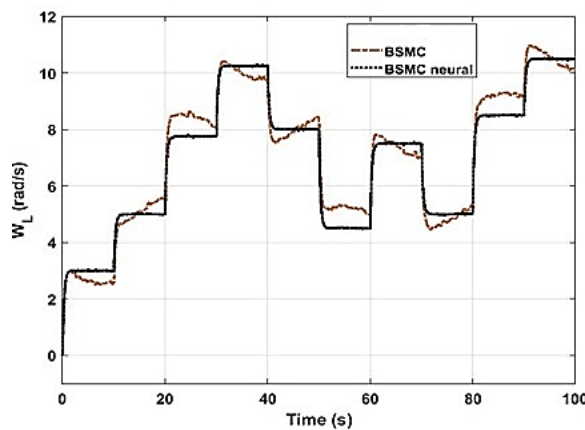


Figure 4. Load angular speed

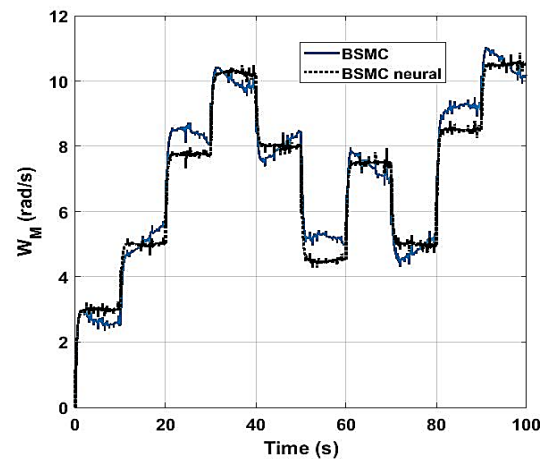


Figure 5. Motor angular speed

Figure 6 displays the load speed errors, with the BSMC method's highest value of roughly 0.9 rad/s. Additionally, the BSMC's number changes following the unidentified load moment, but the neural-based controller's number continuously oscillates within a tolerable range around zero.

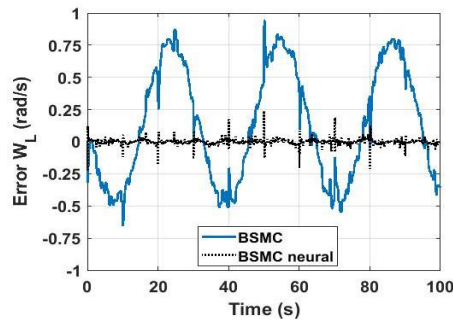


Figure 6. Load angular speed error

The simulation assumes that the load moment is a variable influenced by outside noise from system vibration. Therefore, the load moment is unknown for the model-based controller employing backstepping aggregated with sliding mode control (BSMC). On the other hand, the suggested neural network can approximate a suitable value for unknown components even when the bounded disturbance impacts it, thanks to an adaptive rule developed based on the Lyapunov standard. As a consequence, Figures 7 and 8 show the results of the BSMC in combination with RBF-NN (BSMC neural), which show the improved control performance.

Figures 7 and 8 show the two controllers answers about the reference value. The load angular speed produced by the BSMC neural controller is quite near the target value. However, the system is disturbed and contains an unknown component. Otherwise, when the load speed is sufficiently different from the standard, these negative factors significantly impact the BSMC performance. Similar findings for motor angular speed are shown in Figure 9, which corresponds to the performance.

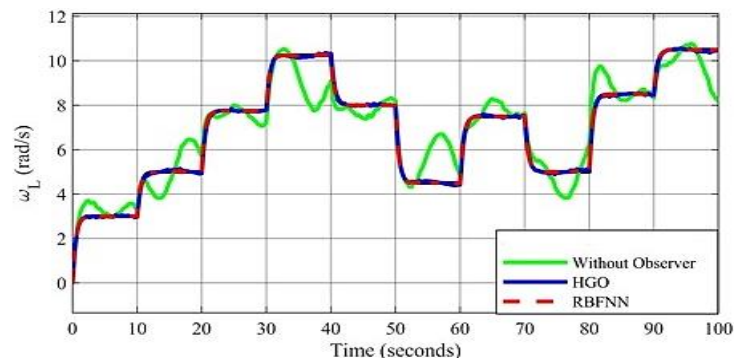


Figure 7. Load angular speed

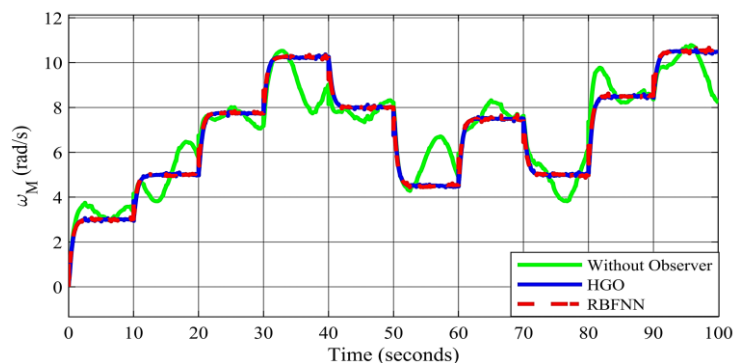


Figure 8. Motor angular speed

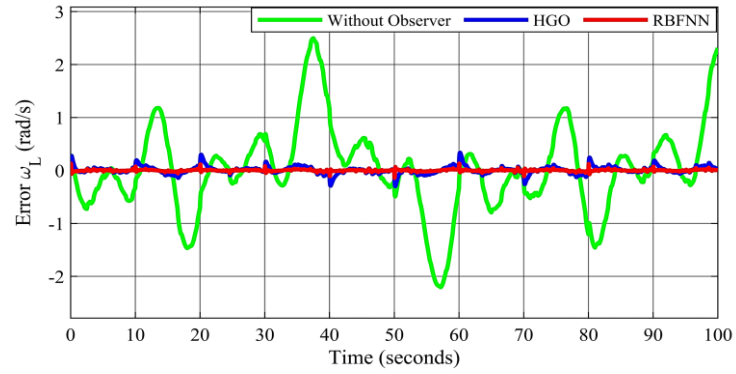


Figure 9. Load angular speed error

Figure 9 displays the load speed errors, with the BSMC method's highest value of roughly 0.9 rad/s. Additionally, the BSMC's number varies following the unidentified load moment, but the BSMC neural-based controller's number consistently oscillates within a tolerable range around zero. Figures 10 and 11 also show motor torque and shaft torque responses. Again, the BSMC neural-based controller reacted to the needed shaft torque in a way that matched load torque estimations and actual value. The neural network's estimated performance is shown in Figure 12. Generally, the output value follows the actual value during the time under consideration. In addition, suitable load moment values are continually produced for the controller to ensure system stability.

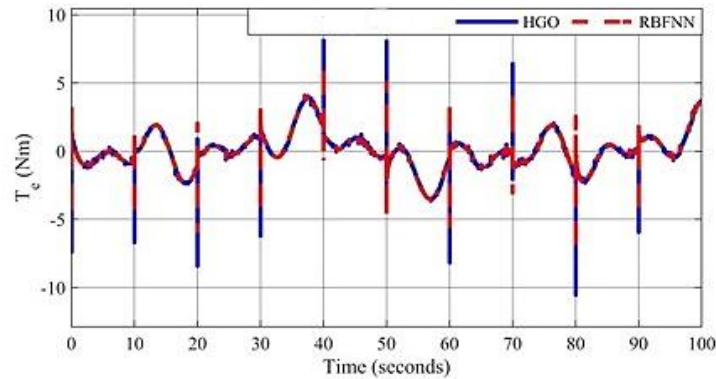


Figure 10. Motor torque

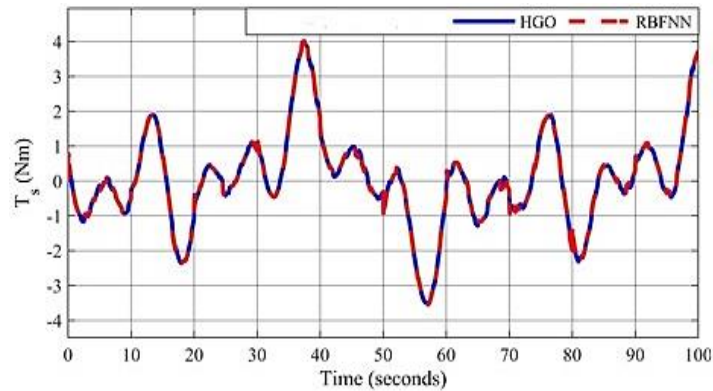


Figure 11. Shaft torque

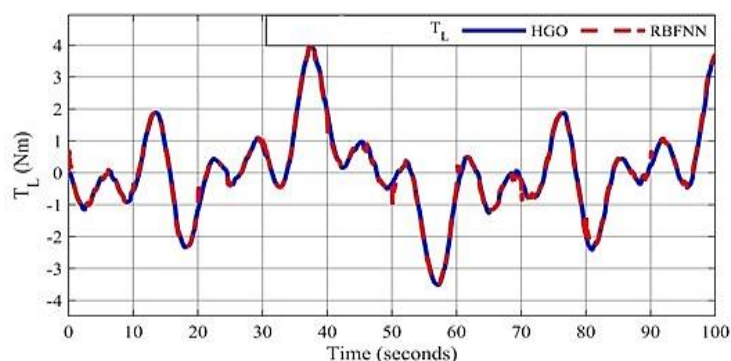


Figure 12. Load torque observers comparison

6. CONCLUSION

This study assumes that the stator currents controller generates the necessary torque at the motor shaft in an electrical drive system with flexible couplings between the motor and the load. In addition, the system's speed control issue is resolved using backstepping-sliding mode control and an RBF-NN observer. This control technique eliminates mismatched noise while regulating the actual angular speed to meet the target angular velocity of the motor and load. The simulation results demonstrate its ability to provide quick and precise reactions and reduce mechanical oscillation in the two-mass system.

ACKNOWLEDGEMENTS

This project study was supported by all researchers and funding from the of the University of Transport and Communications

REFERENCES

- [1] D. Luczak, "Mathematical model of multi-mass electric drive system with flexible connection," *19th International Conference on Methods and Models in Automation and Robotics (MMAR)*, 2014, pp. 590-595, doi: 10.1109/MMAR.2014.6957420.
- [2] C. Ma and Y. Hori, "Backlash Vibration Suppression Control of Torsional System by Novel Fractional Order PID Controller," *IEEE Transactions on Industry Applications*, vol. 124, no. 3, pp. 312-317, 2004, doi: 10.1541/ieejias.124.312.
- [3] G. Zhang and J. Furusho, "Speed control of two-inertia system by PI/PID control," *IEEE Transactions on Industrial Electronics*, vol. 47, no. 3, pp. 603-609, 2000, doi: 10.1109/41.847901.
- [4] I. Hidehiro "PID controller design methods for multi-mass resonance system, PID control for industrial processes," *PID Control for Industrial Processes*, 2018, doi: 10.5772/intechopen.74298.
- [5] K. M. N. C. K. Reddy, B. Rajani, and P. S. Raju, "Control of non linear two mass drive system using ANFIS," *International Journal of Advanced Research in Electrical, Electronics and Instrumentation Engineering (An ISO 3297: 2007 Certified Organization)*, vol. 5, no. 12., pp. 9214-9224, 2016, doi: 10.15662/IJAREEIE.2016.0512014.
- [6] S. Thomsen and F. W. Fuchs, "Flatness based speed control of drive systems with resonant loads," *IECON 2010 - 36th Annual Conference on IEEE Industrial Electronics Society*, pp. 120-125, 2010, doi: 10.1109/IECON.2010.5675188.
- [7] V. T. Ha and N. P. Quang, "Flatness-based control design for two-mass system using induction motor drive fed by voltage source inverter with ideal control performance of stator current," *Proceedings of the VIII International Conference of Students, PhD Students and Young Scientists*, 2019, pp. 39-50, doi: 10.1007/978-3-030-13321-4.
- [8] N. Hoffmann, S. Thomsen and F. W. Fuchs, "Model based predictive speed control of a drive system with torsional loads — A practical approach," *Proceedings of 14th International Power Electronics and Motion Control Conference EPE-PEMC*, 2010, pp. T5-149-T5-156, doi: 10.1109/EPEPEMC.2010.5606693.
- [9] V. T. Ha, L. T. Tan, N. D. Nam, and N. P. Quang, "Backstepping control of two-mass system using induction motor drive fed by voltage source inverter with ideal control performance of stator current," *International Journal of Power Electronics and Drive System*, vol. 10, no. 2, pp. 720-730, 2019, doi: 10.11591/ijpeds.v10.i2.pp720-730.
- [10] M. Mola, A. Khayatian and M. Dehghani, "Backstepping position control of two-mass systems with unknown backlash," *9th Asian Control Conference (ASCC)*, 2013, pp. 1-6, doi: 10.1109/ASCC.2013.6606181.
- [11] M. E. Azzaoui, H. Mahmoudi, K. Boudaraia, "Backstepping control of wind and photovoltaic hybrid renewable energy system," *International Journal of Power Electronics and Drive Systems*, vol. 7, no. 3, pp. 677-686, 2016, doi: 10.11591/ijpeds.v7.i3.pp677-687.
- [12] R. Gunabalan, and V. Subbiah, "Speed sensorless vector control of induction motor drive with PI and fuzzy controller," *International Journal of Power Electronics and Drive System*, vol. 5, no. 3, pp. 315-325, 2015, doi: 10.11591/ijpeds.v5.i3.pp315-325.
- [13] S. Sharma, and A. Gangopadhyay, "Modelling, simulation and speed control of the two-mass drive system," *International Journal of Advanced Research in Electronics and Communication Engineering*, vol. 4, no. 5, 2015, doi: 10.13140/RG.2.2.16892.05762.
- [14] P. H. Shen, and F. J. Lin, "Intelligent backstepping sliding-mode control using RBFN for two-axis motion control system," *IEE Proceedings: Electric Power Applications*, vol. 152, no. 5, pp. 1321-1342, 2005, doi: 10.1007/s42417-021-00333-7.
- [15] S. Q. Liu, J. F. Whidborne and L. He. "Backstepping sliding-mode control of stratospheric airships using disturbance-observer," *Advances in Space Research*, vol. 67, no. 3, pp. 1174-1187, 2021, doi: 10.1016/j.asr.2020.10.047.

- [16] D. Elleuch and T. Damak, "Backstepping sliding mode controller coupled to adaptive sliding mode observer for interconnected fractional nonlinear system," *World Academy of Science, Engineering and Technology International Journal of Mechanical and Mechatronics Engineering*, vol. 7, no. 3, pp. 372-378, 2013, doi: 10.1109/ICCRE.2017.7935036.
- [17] H. Ikeda and T. Hanamoto, "Fuzzy controller of multi-inertia resonance system designed by Differential Evolution," *International Conference on Electrical Machines and Systems (ICEMS)*, 2013, pp. 2291-2295, doi: 10.1109/ICEMS.2013.6713239.
- [18] P. Korondi, H. H. Unot and V. Utkin, "Sliding mode design for two mass system based on reduced order model," *IFAC Proceedings Volumes*, vol. 30, no. 16, pp. 303-308, 1997, doi: 10.1016/S1474-6670(17)42623-1.
- [19] P. Serkies, "Estimation of state variables of the drive system with elastic joint using moving horizon estimation (MHE)," *Bulletin of the polish academy of sciences technical sciences*, vol. 67, no. 5, pp. 883-892, 2019, doi: 10.24425/bpasts.2019.130881.
- [20] K. Szabat, T. T. Van and M. Kamiński, "A modified fuzzy Luenberger observer for a two-mass drive system," *IEEE Transactions on Industrial Informatics*, vol. 11, no. 2, pp. 531-539, 2015, doi: 10.1109/TII.2014.2327912.
- [21] S. Beineke, F. Schutte, and H. Grotstollen, "Comparison of method for estimation and on-line identification in speed and position control loop," *Proceedings of the International Conferences European Power Electronics*, 1997, doi: 10.1109/CCDC.2019.8832705
- [22] J. H. Park, S. H. Huh, S. H. Kim, S. J. Seo and G. T. Park, "Direct adaptive controller for nonaffine nonlinear systems using self-structuring neural networks," *IEEE Transactions on Neural Networks*, vol. 16, no. 2, pp. 414-422, 2005, doi: 10.1109/TNN.2004.841786.
- [23] G. A. Rovithakis, "Robust redesign of a neural network controller in the presence of unmodeled dynamics," *IEEE Transactions on Neural Networks*, vol. 15, no. 6, pp. 1482-1490, 2004, doi: 10.1109/TNN.2004.837782.
- [24] H. A. Talebi, R. V. Patel, and M. Wong, "A neural network based observer for flexible-joint manipulators," *Proceedings. 15th IFAC World Congress Automatic Control*, Barcelona, Spain, 2002, doi: 10.1109/TNN.2005.863458.
- [25] G. Shahgholian, "Modeling and simulation of a two-mass resonant system with speed controller," *International Journal of Information and Electronics Engineering*, vol. 3, no. 5, pp. 448-452, 2013, doi: 10.7763/IJIEE.2013.V3.355.

BIOGRAPHIES OF AUTHORS



Vo Thanh Ha    is a lecturer in the Faculty of Electrical and Electrical Engineering, University of Transport and Communications. She received her B.S degree in Control, and Automation Engineering from the Thai Nguyen University of Technology, Vietnam, in 2002. She received her Master's degree from the Hanoi University of Science and Technology, Vietnam, in 2004. She received a Ph.D. degree from the Hanoi University of Science and Technology, Viet Nam, in 2020, both in Control and Automation Engineering. Her research interests include the field of electrical drive systems, power electronics, and electric vehicles. She can be contacted at email: vothanhha.ktd@utc.edu.vn.



Pham Thi Giang    is a lecturer specializing in automation at the University of Economics and Industry. She received her B.S degree in Electrical Engineering from the University of Transport and Communications in 2020. She received her Master's degree from the Hanoi University of Science and Technology, Vietnam, in 2022. Her research interests include the field of electrical drive systems, power electronics, and electric vehicles. She can be contacted at email: phamthigiang261097@gmail.com.